Threshold Altitude for Bubble Decay and Stabilization in Rat Adipose Tissue at Hypobaric Exposures

Thomas Randsoe and Ole Hyldegaard

Randsoe T, Hyldegaard O. ***Threshold altitude for bubble decay and stabilization in rat adipose tissue at hypobaric exposures.*** **Aviat Space Environ Med 2013; 84:675–83.**

Introduction: Bubble formation during altitude exposures, causing altitude decompression sickness (aDCS), has been referred to in theoretical models as venous gas embolisms (VGE). This has also been demonstrated by intravascular gas formation. Previous reports indicate that the formation of VGE and aDCS incidence increase abruptly for exposures exceeding 40-44 kPa ambient pressures. Further, extravascular micro air bubbles injected into adipose tissue grow transiently, then shrink and disappear while breathing oxygen (F_IO_2 = 1.0) at 71 kPa. At 25 kPa similar air bubbles will grow and stabilize during oxygen breathing without disappearing. We hypothesize that an ambient pressure threshold for either extravascular bubble stabilization or disappearance may be identified between 71 and 25 kPa. Whether extravascular bubbles will stabilize above a certain threshold has not been demonstrated before. ***Methods:*** In anesthetized rats, micro air bubbles (containing 79% nitrogen) of 500 nl were injected into exposed abdominal adipose tissue. Rats were decompressed in 2–35 min to either 60, 47, or 36 kPa and bubbles studied for 215 min during continued oxygen breathing (F_IO_2 = 1). ***Results:*** Significantly more bubbles shrank and disappeared at 60 (14 of 17) and 47 kPa (14 of 15) as compared to bubbles exposed to 36 kPa (3 of 15) ambient pressure. ***Conclusion:*** The results indicate that a threshold causing extravascular bubble stabilization or decay is between 47 to 36 kPa. The results are in agreement with previous reports demonstrating an increase in the formation of VGE and symptoms of aDCS at altitudes higher than 44 kPa ambient pressure.

Keywords: decompression sickness, diving, aviation, space, astronauts, pilots.

ALTITUDE DECOMPRESSION sickness (DCS) is a risk factor during quick decreases in ambient pressure, such as when ascending or cruising at altitude without adequate cabin pressurization, during accidental loss of cabin pressure in commercial or military aircrafts, and during high altitude airdrops (6). Conventional treatment of altitude DCS is oxygen (O_2) breathing combined with fast descent from altitude, eventually followed by recompression during hyperbaric oxygen breathing in a pressure chamber. The purpose is to reduce bubble size by recompression of the gas phase, improve tissue oxygenation, and enhance elimination of dissolved inert gas (5,15).

In order to prevent the supersaturation that causes nitrogen (N_2) bubble formation during low-pressure exposures at altitude, U2 pilots and astronauts prebreathe oxygen prior to ascent, thus exhaling the inert gas saturated into tissue at ground level. However, bubble kinetic models suggest that metabolic gases [i.e., oxygen (O_2), carbon dioxide (CO_2)] and water vapor may also contribute to bubble evolution, and that this effect increases in inverse proportion to the barometric pressure (4,7,23).

In previous reports, micro air bubbles (containing 79% N_2) were injected into adipose tissue of rats decompressed from sea level and held at 71 kPa (12) or 25 kPa (19) (~2,900 and ~10,376 m above sea level) during continued oxygen breathing (F_IO_2 = 1). At 71 kPa, oxygen breathing caused increased growth and prolonged disappearance times of air bubbles when compared to oxygen breathing at 101.3 kPa (sea level) (12). At 25 kPa, bubbles grew even further and stabilized without disappearing (19). By means of preoxygenation, injected micro air bubbles (containing 79% N_2) (19) as well as injected micro oxygen (18) bubbles (containing 0% N_2) were studied in nitrogen-depleted rat adipose tissue at 25 kPa during continuous oxygen breathing (F_IO_2 = 1). We found that preoxygenation enhanced air bubble disappearance and significantly reduced air bubble growth when compared to nonpreoxygenated rats (19), but preoxygenation did not prevent growth of either air or oxygen bubbles (18,19) while at 25 kPa (~10,376 m above sea level). Based on these reports, it is concluded that both N_2 and metabolic gases, O_2 in particular, caused growth and reduced the disappearance rate of air and oxygen bubbles in nitrogen-depleted lipid tissue at 25 kPa. In keeping with this, it is conceivable that bubbles should eventually start to shrink and disappear during oxygen breathing at some point while increasing ambient pressure from 25 to 71 kPa.

Accordingly, we hypothesized that an ambient pressure threshold between 71 and 25 kPa will appear, from which point extravascular air bubbles in adipose tissue either grow and stabilize without disappearing in the observation period, or shrink and disappear within the

From the Laboratory of Hyperbaric Medicine, Department of Anaesthesia, Centre of Head and Orthopaedics, Rigshospitalet, University Hospital of Copenhagen, Copenhagen, Denmark.

This manuscript was received for review in July 2012. It was accepted for publication in January 2013.

Address correspondence and reprint requests to: Thomas Randsoe, Carl Bernhards Vej 9, 2tv, 1817 Frederiksberg C, Denmark; thomasrandsoe@hotmail.com.

DOI: 10.3357/ASEM.3489.2013

observation period, displaying only a transient growth phase. In summary, there will be a threshold point at which, while breathing oxygen, bubble growth will cease, and thereafter either stabilize or shrink and disappear. Therefore, micro air bubbles were injected into rat adipose tissue, after which they were decompressed to and held at 60, 47, or 36 kPa (~4,205, ~6,036, and ~7,920 m above sea level) during continued oxygen breathing ($F_IO_2 = 1$) and bubble monitoring.

METHODS

Animals

The experimental protocol is described in **Fig. 1**. As in previous reports (12,18,19), female Wistar rats weighing 274–315 g with free access to food and water were chosen because of their abundant and transparent abdominal adipose tissue into which bubbles can be injected and clearly viewed through a microscope. The rats were anesthetized with sodium thiomebumal ($0.1\ g \cdot kg^{-1}$) intraperitoneally and buphrenorphine ($0.01–0.05\ mg \cdot kg^{-1}$) subcutaneously. The anesthetized rat was placed supine and fixed to an operating and heating platform on top of an aqueous insulating layer. A cannula was inserted in the trachea (polyethylene tubing-ID 1.5 mm) and a catheter was placed in the left carotid artery for blood pressure registration. It was kept patent by a continuous infusion of nonheparinized denitrogenated saline by means of a syringe pump (Sage Instruments model 341, Freedom, CA) at a rate of $1\ ml \cdot h^{-1}$. To avoid bubble formation during saline infusion at altitude, denitrogenated saline was prepared by means of boiling and subsequent storing in sterile gas-tight syringes with Luer lock (19). Mean arterial blood pressure (MAP) was measured throughout the experiment by means of a pressure transducer from Edwards Lifesciences™ (Irvine, CA) placed inside the chamber. A thermometer placed in the vagina measured body temperature. The vaginal thermometer was connected to a thermostat preset at 37°C to maintain a body temperature of 37°C during decompression exposures, giving a chamber temperature at 32–36°C. A continuous real-time record of temperature and MAP was obtained on a PC via a Picolog® data collection software.

The abdomen was opened in the midline and the abdominal adipose tissue was exposed. A Licox™ oxygen microcatheter and a Licox thermoprobe were placed inside the adipose tissue for continuous measurements of tissue oxygen partial pressure ($P_{tissue}O_2$) and temperature. In all groups $P_{tissue}O_2$ values were registered every 15 min during the observation period. With a 2.0-mm ID cannulla, the cecum was perforated and the cannulla left in situ to function as drainage for expanding bowel gases during decompression. The rat was then transferred to the pressure chamber attached to the operating and heating platform. Once inside the chamber the tracheal cannula was connected to the T-shaped tube in the chamber breathing system and the connections for MAP registration and rat vaginal thermometers were made. A glass micropipette mounted on a 5-μl Hamilton syringe was guided to the tissue. Two to six air bubbles with a volume of 500 nl were then injected superficially and widely separated (i.e., in order to exclude any direct gas exchange between adjacent bubbles) into the adipose tissue using a UMP2™ ultra precision pump from WPI© (Worcester, MA). The numbers of bubbles injected were limited by the surface area of the exposed adipose tissue, partly by assuring their separation from larger blood vessels and nearby peristaltic movements, which could otherwise distort the microscopic picture during

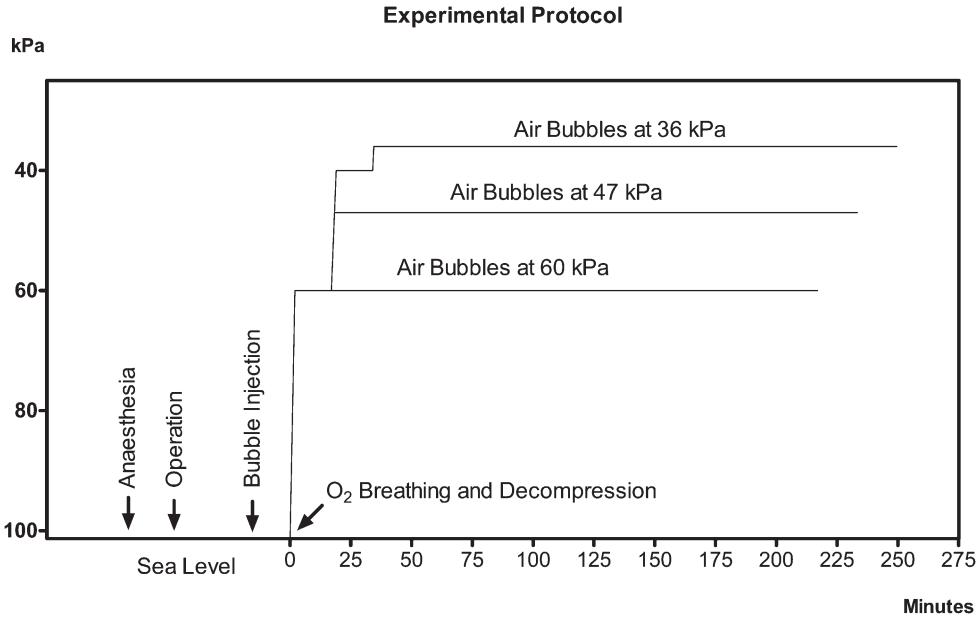

Fig. 1. Experimental protocol. Time spent during the different experimental procedures and bubble injection at sea level followed by time spent at the different barometric exposures. All rats breathed oxygen ($F_IO_2 = 1$) from the moment of decompression until termination of the experiment. Time from decompression to first bubble observation at altitude depended on the decompression profile for the respective group.

the observation period. Injection time lasted 8-15 min and subsequently the exposed tissue was covered with a gas impermeable Mylar membrane and a polyethylene membrane to prevent evaporation. The principle of the injection technique has been described previously (13).

In total 47 injected bubbles were studied in 15 rats with 5 rats in each group; the 5 rats decompressed to 60 kPa had a total amount of 17 bubbles injected while the 5 rats decompressed to, respectively, 47 and 36 kPa had a total amount of 15 bubbles injected in each group. The experimental use of anesthetized rats was approved by a Government-granted license from the Danish Animal Ethical Committee at the department of justice and conducted in agreement with the Declaration of Helsinki II.

Procedure

The upper steel lid of the pressure chamber was attached and a stereomicroscope was positioned over the viewing port in the chamber. A video camera attached to the stereomicroscope recorded the microscopic picture of the bubbles and the recording was transferred to a DVD recorder. In all rats the predecompression bubble dimensions were obtained at 101.3 kPa (sea level) with the rats' breathing system switched to oxygen ($F_IO_2 = 1$) at the moment of decompression to, respectively, 60, 47, and 36 kPa (~4,205, ~6,036, and ~7,920 m above sea level). Decompression to altitude was performed over a period of 2–35 min with two stops of 15 min duration at 60 and 40 kPa in order to prevent manifest DCS. Total decompression time for the respective groups was: 60 kPa, 2 min; 47 kPa, 18 min and 18 s with a 15-min stop at 60 kPa; 36 kPa, 34 min and 32 s with a 15-min stop at 60 and 40 kPa (see Fig. 1). Once at altitude, individual bubble dimensions were recorded at every 2–5 min for up to 215 min as the maximal bubble observation time or until bubbles disappeared from view, at which point the rat was recompressed to 101.3 kPa. The rats continued oxygen breathing throughout the entire experiment. After recompression back to 101.3 kPa, the rat was removed from the pressure chamber and placed under the operating binoculars. With the rat still attached to the operating and heating platform, the thorax and abdomen were opened for a microscopic scan for intra- or extravascular gas formation before the rat was euthanized by means of exsanguination.

Equipment

Decompression was performed in a specially designed pressure chamber with a horizontal viewing port 16 cm in diameter. The anesthetized rat was placed supine on a circular plate that could be removed from the pressure chamber and serve as an operating platform. The platform also contained a built-in heating system, which was controlled by a vaginal thermometer maintaining body temperature at an average of 37°C [see Fig. 1 in Hyldegaard et al. (11)]. The breathing gas was supplied continuously at a pressure slightly above chamber pressure and flowed inside the chamber through an 8-mm ID silicone tube with a small latex rubber-breathing bag and a T-connection for the rat's tracheal cannula. The tube was connected to the exhaust outlet via a specially designed overboard dump valve. The breathing, pressurizing, and chamber heating system has been described in a previous report (12).

Bubbles were observed through the chamber window at 40× magnification by means of a Leica™ Wild M10 stereomicroscope (Wetzler, Germany) with a long focal-length objective. Two flexible fiber optic light guides, attached to a Volpo Intralux 5000 lamp (Schlieren, Switzerland), illuminated the bubble field. A Kappa™ CF 15/2 color video camera was fitted to the microscope, and the field was displayed on a TV screen and recorded on a DVD recorder [Panasonic™ DMR-DH86; see Fig. 1 in Hyldegaard et al. (11)]. The recording was then transferred to a computer in order to capture real-time images using the NIH Image version 1.61 program (20) and the visible surface area of the bubbles was calculated by means of automated planimetry. The computer program was calibrated by comparison with a metal rod of 200 μm in diameter placed on top of the adipose tissue in the observed field.

Statistical Analysis

Bubbles were analyzed with respect to bubble "growth time," defined as time of observed bubble growth from first observation at altitude until time of maximal bubble size was measured. Similarly bubbles were measured with respect to bubble "disappearance time," defined as first observation at altitude until bubbles disappeared. If a bubble did not disappear within the observation period, the end point was recorded as 215 min as the last time of observation. Bubble growth time and disappearance time is expressed in minutes and mean values are given ± SD. Bubbles were also analyzed with respect to mean "growth rate" ($mm^2 \cdot min^{-1}$) from the time of first observation at altitude until maximal bubble size was measured. If a bubble did not grow but shrank while at altitude, it was given a negative value, indicating shrinkage. Bubble "disappearance rate" was expressed as the mean net disappearance rate (mm^2 x min^{-1}), i.e., the slope of a line from the first measured bubble size during observation at altitude to disappearance of the bubble. If a bubble did not disappear, the mean net disappearance rate was calculated as the slope of the line connecting the first observation at altitude with the last observation. If a bubble did not shrink but grew it was given a negative value, indicating growth. Mean values of calculated bubble growth rates and disappearance rates are given ± SD.

To examine whether the differences between two mean values of calculated bubble growth times, disappearance times, growth rates, or disappearance rates were different from zero, test for normality by means of the Kolmogorov and Smirnov test followed by either parametric one-way analysis of variance (ANOVA) or nonparametric ANOVA (Kruskal-Wallis Test) was performed on the difference between mean values in the different treatment groups. The difference between mean values in the treatment groups were then analyzed by

use of the Bonferroni Multiple Comparisons Test of means between groups (22) or Dunn's test (1,2,9). When several bubbles were studied in one animal, their mean value was used in the statistical comparison.

Furthermore, bubbles were analyzed with respect to their mean "growth ratio" using a nonparametric analysis of variance ANOVA (Kruskal-Wallis Test). Bubble growth ratio was calculated as maximal measured bubble size in the observation period divided with the first observed bubble size in the observation period at altitude (1,2,9). Bubbles were also compared with respect to "bubbles disappeared" or "bubbles not disappeared" in the observation period by means of a contingency table using Fishers Exact test (1,2,9).

The mean values of $P_{tissue}O_2$ (mmHg) measurements at altitude were calculated for each animal. To examine whether the difference between two mean values of $P_{tissue}O_2$ measurements were different from zero, test for normality by means of the Kolmogorov and Smirnov test followed by one-way ANOVA was performed on the difference between mean values in the different treatment groups. The difference between mean values of the various treatment groups were then analyzed by use of Bonferroni Multiple Comparisons Test of means between groups (1,2,9). Statistical analysis by means of ANOVA (Kruskal-Wallis Test) was performed between groups with respect to possible differences in the size of injected bubbles and first observed bubble size at altitude. For all comparisons $P < 0.05$ was regarded as the criteria for significance.

RESULTS

Rats were breathing spontaneously while connected to the overboard dump valve system during decompression and at altitude and all rats seemed unaffected with respect to blood pressure measurements when decompression was initiated and at altitude. When the abdominal and thoracic cavities of the 15 recompressed rats were opened for microscopic examination before exsanguination, no bubbles were visible in the veins. The thermostatically controlled rat temperatures were stable at 37°C, except from short fluctuations at an interval of 34–37°C during the operation and decompression phase. During decompression, some bowel expansion was observed. Peristaltic movements were lively and visible throughout the experiment. During the observation period, adipose tissue perfusion in the smaller vessels with a diameter of 10–15 μm was clearly visible and seemed unaffected throughout the experiment.

Before decompression was initiated, MAP was stable and in the range of 175–225 mmHg as the most frequent interval for all groups. During the decompression period and at altitude, rats had a slowly decreasing tendency in the MAP, with the most frequent interval at the range of 150–200 mmHg in the end of the observation period.

During oxygen breathing at 60 kPa ($N = 5$ rats), 16 of 17 bubbles initially grew at a mean growth rate of 4.3×10^{-3} mm$^2 \cdot$ min^{-1} ($\pm 3.2 \times 10^{-3}$) and mean growth ratio of 1.51 ($\pm$ 0.46) (see **Fig. 2** and **Table I**). Bubbles grew transiently for a period of 20–64 min [mean 44 min ($\pm$ 14)], after which they stabilized or began to shrink slowly; 14 bubbles disappeared within 116–203 min [mean 160 ($\pm$ 36 min)], of which 1 bubble shrank consistently without a growth phase while 3 bubbles stabilized with a slowly shrinking tendency toward the end of the observation period. When bubbles started to shrink, the mean net disappearance rate for all bubbles was 2.0×10^{-3} mm$^2 \cdot$ min^{-1} ($\pm 0.9 \times 10^{-3}$). $P_{tissue}O_2$ mean was 180 mmHg ($\pm$ 9).

During oxygen breathing at 47 kPa ($N = 5$ rats), 14 of 15 bubbles initially grew at a mean growth rate of 3.4×10^{-3} mm$^2 \cdot$ min^{-1} ($\pm 4.7 \times 10^{-3}$) and mean growth ratio of 0.89 ($\pm$ 0.5) (see **Fig. 3** and Table I). Bubbles grew transiently for a period of 4-97 min [mean 23 min ($\pm$ 24)], after which they stabilized or began to shrink slowly; 14 bubbles disappeared within 122–214 min [mean 178 ($\pm$ 30 min)], of which 1 bubble shrank consistently without a growth phase while 1 bubble stabilized with a shrinking tendency toward the end of the observation period. When bubbles started to shrink, the mean net disappearance rate for all bubbles was 4.4×10^{-3} mm$^2 \cdot$ min^{-1} ($\pm 0.7 \times 10^{-3}$). $P_{tissue}O_2$ mean was 146 mmHg ($\pm$ 20).

During oxygen breathing at 36 kPa ($N = 5$ rats), 13 of 15 bubbles initially grew at a mean growth rate of 5.6×10^{-3} mm$^2 \cdot$ min^{-1} ($\pm 2.4 \times 10^{-3}$) and mean growth ratio of 1.03 ($\pm$ 0.34) (see **Fig. 4** and Table I). Bubbles grew transiently for a period of 6–107 min [mean 32 min ($\pm$ 19)], after which they stabilized or began to shrink slowly; 3 bubbles disappeared within 149–207 min [mean 175 min ($\pm$ 30 min)], of which 2 bubbles only had a shrinking phase while 12 bubbles stabilized with a slowly shrinking tendency toward the end of the observation period. When bubbles started to shrink, the mean net disappearance rate for all bubbles was 3.7×10^{-3} mm$^2 \cdot$ min^{-1} ($\pm 1.5 \times 10^{-3}$). $P_{tissue}O_2$ mean was 99 mmHg ($\pm$ 14) (see **Fig. 5**).

ANOVA showed no significant differences between groups with respect to the size of the injected bubbles [$F(2,12) = 0.49$, $P = 0.62$] prior to decompression, while there was significant difference between all groups regarding first observed bubble size at altitude [$F(2,12) = 21.4$, $P < 0.0001$]. ANOVA followed by multiple comparisons among the groups showed no significant difference between the groups regarding growth time [$F(2,12) = 1.4$, $P = 0.3$] or growth rate [$F(2,12) = 0.5$, $P = 0.6$]. ANOVA testing showed that net disappearance rates were different [$F(2,12) = 6.4$, $P = 0.01$]. Net disappearance rate was significantly faster at 47 kPa when compared to 60 kPa ($P < 0.05$), while the observed difference when comparing 60 with 36 kPa altitude levels did not quite reach statistical difference at the $P < 0.05$ level ($0.1 > P > 0.05$). There was no significant difference when comparing 47 with 36 kPa. When bubbles disappeared, there were no differences in bubble disappearance time among groups [$F(2,19) = 0.4$, $P = 0.7$]. ANOVA showed that bubble growth ratio was not significantly different among groups [$F(2,12) = 2.8$, $P = 0.1$].

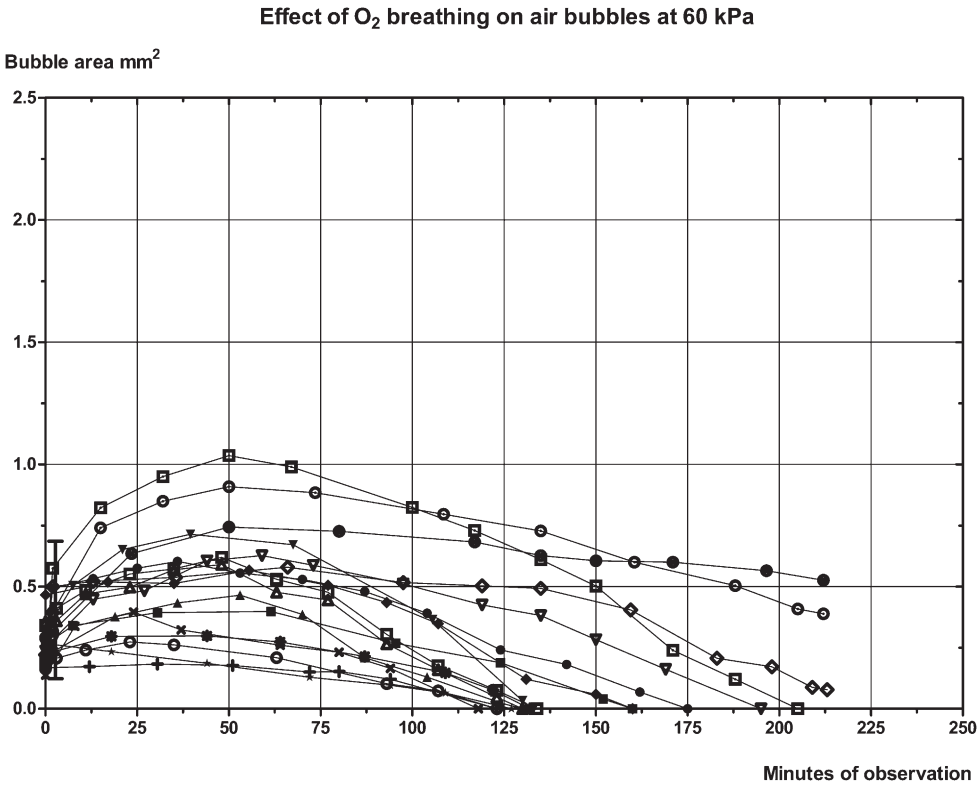

Fig. 2. Effect of oxygen breathing ($F_IO_2 = 1$) on injected micro air bubbles in adipose tissue at 101.3 kPa (sea level pressure) followed by decompression to 60 kPa (~4,205 m above sea level) in 2 min. Oxygen breathing took place from the first point on each curve. Each curve represents 1 bubble. Vertical bar indicates time of arrival at 60 kPa.

Fishers exact test showed that the number of bubbles disappearing in the observation period at 36 kPa was significantly different from both 60 ($P < 0.001$) and 47 kPa ($P < 0.0001$). There were no differences when comparing 60 with 47 kPa. ANOVA showed that mean $P_{tissue}O_2$ values were different [$F(2,17) = 46.23$, $P < 0.0001$]. Bonferroni post hoc analysis showed that mean $P_{tissue}O_2$ values were significantly higher at 60 kPa than at both 47 ($P < 0.01$) and 36 kPa ($P < 0.001$), while values were significantly higher at 47 kPa than at 36 kPa ($P < 0.001$).

DISCUSSION

The purpose of the present experiment was to establish an altitude threshold, at which point extravascular

TABLE I. AIR BUBBLE GROWTH RATE, TIME, RATIO, NET DISAPPEARANCE RATE, $P_{TISSUE}O_2$, AND BUBBLE DISAPPEARANCE/STABILIZATION IN RAT ADIPOSE TISSUE AT 60, 47, OR 36 kPa ALTITUDE EXPOSURES DURING OXYGEN BREATHING.

Treatment Group	Growth Rate ($mm^2 \cdot 10^{-3} \cdot min^{-1}$)*	Growth Time (min)*	Growth Ratio*	Net Disappearance Rate ($mm^2 \cdot 10^{-3} \cdot min^{-1}$)*	$P_{tissue}O_2$** (mmHg)*	Bubbles disappeared / stabilized
Air bubbles at 60 kPa	$4.3 \times 10^{-3} \pm 3.2 \times 10^{-3}$	44 ± 14	1.51 ± 0.46	$2.0 \times 10^{-3} \pm 0.9 \times 10^{-3}$	180 ± 9[3]	14 of 17***
$N = 5$ Animals $N = 17$ Bubbles						3 of 17****
Air bubbles at 47 kPa	$3.4 \times 10^{-3} \pm 4.7 \times 10^{-3}$	23 ± 24	0.89 ± 0.5	$4.4 \times 10^{-3} \pm 0.7 \times 10^{-3}$ [1]	146 ± 20[4]	14 of 15***
$N = 5$ Animals $N = 15$ Bubbles						1 of 15****
Air bubbles at 36 kPa	$5.6 \times 10^{-3} \pm 2.4 \times 10^{-3}$	32 ± 19	1.03 ± 0.34	$3.7 \times 10^{-3} \pm 1.5 \times 10^{-3}$	99 ± 14	3 of 15[2],***
$N = 5$ Animals $N = 15$ Bubbles						12 of 15****

* Values are means ± SD.
** $P_{tissue}O_2$: Tissue Partial Pressure of O_2
*** Bubbles disappearing
**** Bubbles stabilizing
[1]Air bubble net disappearance rate at 47 kPa different from air bubble net disappearance rate at 60 kP ($P < 0.05$).
[2]Number of bubbles disappearing/stabilizing at 36 kPa different from number of bubbles disappearing/stabilizing at 60 kPa ($P < 0.001$) and 47 kPa ($P < 0.0001$).
[3]$P_{tissue}O_2$ at 60 kPa different from $P_{tissue}O_2$ at 47 ($P < 0.01$) and 36 kPa ($P < 0.001$).
[4]$P_{tissue}O_2$ at 47 kPa different from $P_{tissue}O_2$ at 36 kPa ($P < 0.001$).

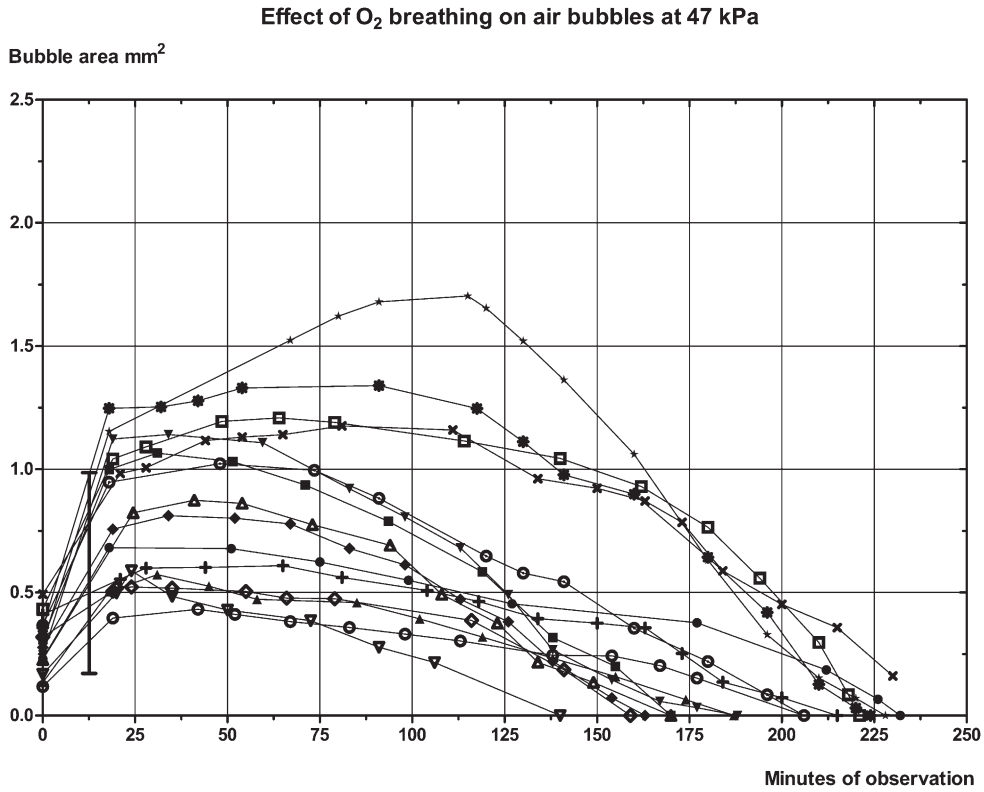

Fig. 3. Effect of oxygen breathing ($F_IO_2 = 1$) on injected micro air bubbles in adipose tissue at 101.3 kPa (sea level pressure) followed by decompression to 47 kPa (~6,036 m above sea level) in 18 min and 18 s with one stop of 15 min at 60 kPa. Oxygen breathing took place from the first point on each curve. Each curve represents 1 bubble. Vertical bar indicates time of arrival at 47 kPa.

air bubble growth and stabilization are halted and bubbles start to shrink and disappear during continued oxygen breathing at altitude. According to Boyles Law, bubbles initially increased in volume with a factor 101.3/60 = 1.68, 101.3/47 = 2.15, and 101.3/36 = 2.81, corresponding to the immediate effect of decompression from 101.3 kPa to 60, 47, and 36 kPa absolute pressure. While decompressed, bubbles grew irregular in shape due to the expanding gas and the tissue elasticity of the adipose tissue. Accordingly, bubble volumes could not be calculated by measuring bubble diameters. Therefore, bubble size was measured as visible surface area, a method that adds an uncertainty to our results. However, since bubbles initially grew while at altitude, an increase in bubble area should only imply an even greater growth of bubble volume.

Assuming that the nitrogen partial pressure in tissue ($P_{tissue}N_2$) equilibrates with that of the injected microbubble ($P_{bubble}N_2$), and that there is no pulmonary diffusion limitation or physiological shunt, then the $P_{bubble}N_2$ would be equal to $P_{tissue}N_2$, which is equal to the alveolar N_2 partial pressure (P_AN_2) (24). Subtracting the alveolar partial pressures of oxygen, carbon dioxide, and water vapor, the $P_{bubble}N_2 = 76$ kPa (28). When switched to oxygen breathing just before decompression, $P_{tissue}N_2$ is reduced through exhalation at a nitrogen tissue halftime ($T_{1/2}N_2$) of 29 min, measured by means of radioactive Xe^{133} washout in exactly the same kind of anesthetized rats, since the tissue perfusion is 0.105 ml blood $\cdot$ g^{-1} $\cdot$ min^{-1} and the partition coefficient (λ) for nitrogen between 85% lipid and blood is 0.066/0.0148 for rat abdominal adipose tissue (14,26). Therefore, the $P_{tissue}N_2$ at the beginning of the observation period, i.e., once at the predefined altitude pressure, will depend on the period of oxygen breathing during the respective decompression profiles (see Fig. 1). An oxygen breathing period is necessary to prevent fatal altitude DCS as described in our previous report (19). When the rat is decompressed to 60 kPa in 2 min and assuming the same prerequisites as mentioned above, the P_AN_2 will be approximately 42 kPa due to the effect of the immediate decompression. Accordingly, the $P_{tissue}N_2$ supersaturation will be approximately 34 kPa, disregarding the short period of oxygen breathing during decompression. Similarly, when decompressed to 47 kPa in 18 min, the period of oxygen breathing is close to half $T_{1/2}N_2$, causing a $P_{tissue}N_2$ supersaturation of approximately 33 kPa. When decompressed to 36 kPa in 34.5 min, the period of oxygen breathing is close to 1 $T_{1/2}N_2$, causing a $P_{tissue}N_2$ supersaturation of approximately 27 kPa. It hereby follows that as ambient pressure is reduced, the introduction of oxygen breathing during decompression will result in minor changes in $P_{tissue}N_2$ supersaturation (range from 34 to 27 kPa) relative to the greater change in ambient pressure. The fact that the injected micro air bubbles in the present experiment behave almost similarly with respect to bubble growth time, rate, and ratio at either 60, 47, or 36 kPa ambient pressure may partly

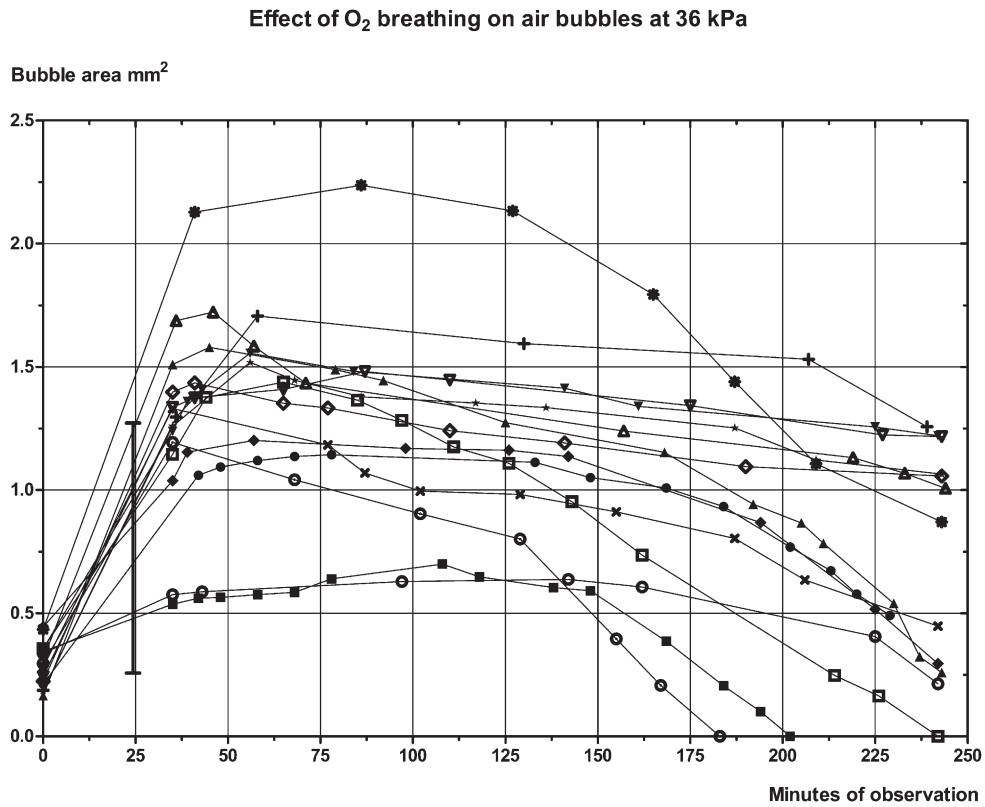

Fig. 4. Effect of oxygen breathing (F_IO_2 = 1) on injected micro air bubbles in adipose tissue at 101.3 kPa (sea level pressure) followed by decompression to 36 kPa (~7,920 m above sea level) in 34 min and 32 s with two stops of 15 min at 60 kPa and 40 kPa. Oxygen breathing took place from the first point on each curve. Each curve represents 1 bubble. Vertical bar indicates time of arrival at 36 kPa.

be explained by the same degree of $P_{tissue}N_2$ supersaturation (difference from 1 to 7 kPa) as described above. However, decompression to 36 kPa ambient pressure caused significantly more injected micro air bubbles to stabilize without disappearing in the observation period as compared to decompression to 60 or 47 kPa ambient pressures, an effect seen in spite of the smaller $P_{tissue}N_2$ supersaturation at 36 kPa. Once decompressed, most bubbles were observed to grow transiently, irrespective of ambient pressure, due to the $P_{tissue}N_2$ supersaturation as described above. Nonetheless, bubble disappearance rate was significantly faster at 47 kPa as compared to 60 kPa, whereas the difference between 60 kPa and 36 kPa did not quite reach statistical significance ($0.1 > P > 0.05$). However, the observed variability in bubble growth and stabilization, as well as bubble shrinkage and disappearance rates at the different altitude levels (see Fig. 2-4), also depend on local alterations in adipose tissue blood flow and oxygen metabolism along with an impaired effect of the oxygen window (8,24), so inconsistency is to be expected. During decompression to altitude, several mechanisms may explain the current observations.

1. The immediate effect of decompression is bubble expansion according to Boyle's law. In the present experiments, bubbles grew with a factor of 1.68–2.81 during decompression, thereby increasing the bubble surface area. An increase in surface area creates a larger tissue to bubble interface, facilitating gas diffusion across the bubble wall (23). For a given diffusion gradient, each gas will have a higher flux through the larger surface area (23), which in accordance with Fick's first law of diffusion (8,23,25) and the greater solubility and permeability [i.e., the product of the diffusion coefficient and solubility coefficient (26)] of oxygen than that of nitrogen in a lipid tissue, further enhance bubble growth at altitude.
2. When nitrogen enters the bubble, the oxygen content is diluted, promoting diffusion of oxygen from arterial blood (F_IO_2 = 1.0) to the bubble, which further contributes to bubble growth. Additionally, as previously shown in Randsoe and Hyldegaard and Randsoe et al. (18,19), an oxygen partial pressure difference between arterial blood and bubbles of 0.8 + $P_{bubble}N_2$ kPa exist, further supporting bubble growth. However, the flux of nitrogen going out of the bubble will obey Fick's first law of diffusion (8,23,25) and, as nitrogen is slowly lost by diffusion from the bubble and tissue during continued oxygen breathing, driven by the nitrogen partial pressure difference between bubble, tissue, and blood, the oxygen partial pressure in the bubble increases, promoting outwards diffusion of oxygen to the surrounding tissue. At the end of the observation period, up to 8 $N_2T_{1/2}$ have elapsed and $P_{bubble}N_2$ and $P_{tissue}N_2$ would, therefore, be close to zero (8 $N_2T_{1/2}$ = $P_{tissue}N_2$ < 0.4%). As nitrogen disappears, the oxygen partial pressure difference between P_aO_2 and $P_{bubble}O_2$ is reduced toward 0.8 kPa (18,19), at which point less oxygen is now received from the blood than what is given off to the surrounding metabolizing tissue. If $P_{bubble}N_2$ is regarded as zero, the $P_{bubble}O_2$ can be calculated according to equation 2 and 4 in Randsoe and Hyldegaard (18), giving a $P_{bubble}O_2$ of 47.6, 34.6, and 23.6 kPa at 60, 47, or 36 kPa ambient pressures. With reference to the measured mean $P_{tissue}O_2$ (see Fig. 5), the gradient between $P_{bubble}O_2$ and $P_{tissue}O_2$ can be calculated; since $P_{tissue}O_2$ = 180 mmHg at 60 kPa ambient pressure (see Fig. 5) and 1 kPa equals 7.5 mmHg, $P_{bubble}O_2 - P_{tissue}O_2$ = 47.6 kPa – 24 kPa = 23.6 kPa. The same calculation applies for ambient pressures at 47 and 36 kPa, giving a stepwise declining gradient from 23.6 to 15.1 and 10.4 kPa at 60, 47, and 36 kPa ambient pressures, respectively, explaining bubble shrinkage.
3. As the P_aO_2 is reduced during decompression to altitude, it is conceivable that the vasoconstrictor effect of oxygen is less pronounced

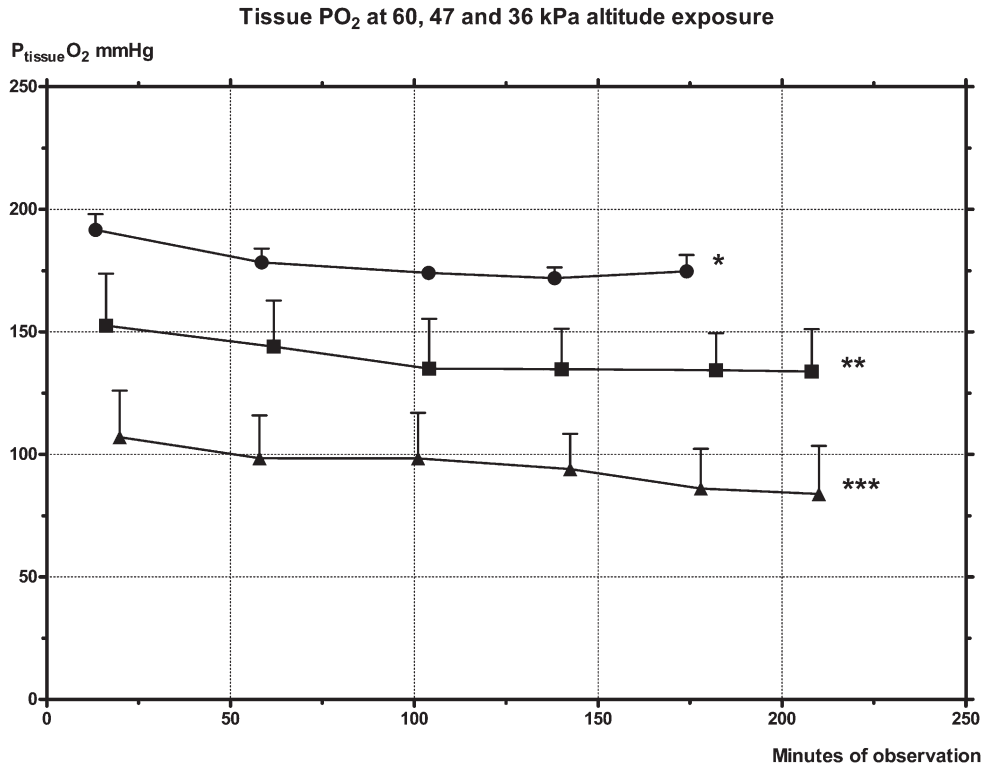

Fig. 5. Effect of oxygen breathing ($F_IO_2 = 1$) and decompression on adipose tissue oxygen partial pressure ($P_{tissue}O_2$). Each curve represents mean $P_{tissue}O_2 \pm$ SD (mmHg) during the observation period at altitude. *$P_{tissue}O_2$ at 60 kPa. **$P_{tissue}O_2$ at 47 kPa. ***$P_{tissue}O_2$ at 36 kPa.

during low pressure exposures, which would favor the microcirculation at altitude and further contribute to bubble growth.

4. If the sum of alveolar partial pressures in normobaric conditions is 101.3 kPa, the total gas tension in venous blood is 93.5 kPa. Thus, there is an "inherent unsaturation" (10) at a difference of 7.8 kPa, i.e., the "oxygen window" (3). However, the effect levels off as barometric pressure decreases in the hypobaric range because the oxygen window (10) between venous blood and alveolar gas phase is reduced as P_AO_2 decreases, since $P_{tissue}O_2$ (see Fig. 5) falls in proportion to the reduced pressure, while PH_2O and $P_{tissue}CO_2$ remains constant, the latter as long as hypoxia with subsequent hyperventilation is avoided (24). Further, as demonstrated by Foster et al. (8), the increased amount of dissolved tissue oxygen in the bubble region during sustained oxygen breathing at altitude will decrease the oxygen window between bubble and tissue, tending to slow the rate of bubble decay (see Fig. 4).
5. The bubble stabilization observed with increasing altitude is in agreement with our previous experiments, where both air (19) and oxygen (18) bubbles were found to grow and stabilize while at 25 kPa ambient pressure, despite complete nitrogen depletion from the tissue through preoxygenation. The effect was ascribed to the contribution of metabolic gases, oxygen in particular, as well as carbon dioxide and water vapor and is consistent with bubble kinetic models (4,7,23) predicting that the internal fraction of metabolic gases in the bubble increases with decreasing barometric pressure, thereby enhancing bubble growth.

It is an obvious limitation to the present experiment that only tissue bubbles were studied since bubbles during DCS are known to form in the intravascular compartment. However, in a previous report by Webb et al. (27), a threshold for DCS at staged altitude was found at 57 kPa (~4,603 m above sea level) for first appearance of Doppler-detectable precordial VGE and approximately 48-44 kPa (~5,872 – 6,503 m above sea level) for 5% DCS incidence with 95% confidence interval (27). $F_IO_2 = 1$ beginning with ascent (ascent rate 1,524 m · min $^{-1}$) and at sojourn, but with zero preoxygenation. At 44 kPa VGE incidence was ~50%; however, the DCS incidence was ~50% at 40 kPa (7,183 m above sea level) and climbed abruptly thereafter to 90% at 37.6 kPa (7,617 m above sea level) (27). Further, in vitro experiments by Olson and Krutz found a substantial increase in bubble size between 50.6 and 37.6 kPa (5,486–7,620 m above sea level) relative to growth below or above those altitudes (16). Accordingly, the sudden increase in DCS incidence at 44 kPa (27) and abrupt increase in bubble growth between 50.6 and 37.6 kPa (16) correspond to the observed significant changes of bubble stabilization going from 47 to 36 kPa ambient pressure in the present experiment. It is concluded that the level of threshold altitude at which point extravascular bubbles either disappear or stabilize is within the interval from 47 to 36 kPa (~6,036 to ~7,920 m above sea level).

Recently, intravenously administered perfluorocarbon (PFC) emulsions, due to its ability of dissolving respiratory gases, thereby improving oxygen delivery to tissues and transport of nitrogen from tissues to the lungs, have been used experimentally in treating DCS after air diving (21). Further, PFC emulsions have been shown to cause faster elimination of extravascular air bubbles in adipose tissue during normobaric oxygen breathing using a model similar to the present experiments (17). Similarly, nitrogen oxide (NO) donors have proven beneficial in preventing DCS from air diving, supposedly caused by increased blood flow rate or removal of micronuclei precursors (29). During altitude

DCS, it is reasonable to assume that both PFC and NO would favor tissue bubble disappearance through an increased transport capacity of nitrogen by means of PFC circulating in blood as well as through the augmented tissue perfusion caused by NO elicited vasodilatation. However, in keeping with the present results and our previous reports (17–19), it seems conceivable that the increased oxygen transport by PFC and NO could cause an undesirable increase in air bubble growth in hypobaric conditions. Accordingly, further experiments testing the effect of combined oxygen breathing and PFC and a NO donor at high altitude exposures seem warranted.

ACKNOWLEDGMENTS

The assistance of laboratory technician Mr. Ian Godfrey for his help in the manufacture of the glass micropipettes is greatly appreciated. Thanks are given to senior Hyperbaric Supervisor Michael Bering Sifakis in assisting us with chamber support and maintenance. The Lundbeck Foundation, The Laerdal Foundation for Acute Medicine, and Rigshospitalets Forskningsudvalg supported the present work.

Authors and affiliations: Thomas Randsoe, M.D., and Ole Hyldegaard, M.D., Ph.D., D.M.Sc., Laboratory of Hypberbaric Medicine, Department of Anaesthesia, Centre of Head and Orthopaedics, Rigshospitalet, University Hospital of Copenhagen, Copenhagen, Denmark.

REFERENCES

1. Altman DG. Practical statistics for medical research. London: Chapman and Hall; 1991.
2. Armitage P, Berry G, Matthews JNS. Statistical methods in medical research. Oxford: Blackwell Scientific; 1987.
3. Behnke AR. The isobaric (oxygen window) principle of decompression. In: The New Thrust Seaward: Transactions of the Third Marine Technology Society Conference and Exhibit; San Diego, CA. Washington, DC: Marine Technology Society; 1967.
4. Burkard ME, Van Liew HD. Simulation of exchanges of multiple gases in bubbles in the body. Respir Physiol 1994; 95:131–45.
5. Dart TS, Butler W. Towards new paradigms for the treatment of hypobaric decompression sickness. Aviat Space Environ Med 1998; 69:403–9.
6. Foster PP, Butler BD. Decompression to altitude: assumptions, experimental evidence, and future directions. J Appl Physiol 2009; 106:678–90.
7. Foster PP, Conkin J, Powell MR, Waligora JM, Chhikara RS. Role of metabolic gases in bubble formation during hypobaric exposures. J Appl Physiol 1998; 84:1088–95.
8. Foster PP, Feiveson AH, Glowinski R, Izygon M, Boriek AM. A model for influence of exercise on formation and growth of tissue bubbles during altitude decompression. Am J Physiol Regul Integr Comp Physiol 2000; 279:R2304–16.
9. Graph-Pad [computer program]. Instat version 3.06 for Windows. San Diego, CA: GraphPad Software, Inc.; 2003.
10. Hills B. Decompression sickness. New York: John Wiley & Sons; 1977.
11. Hyldegaard O, Kerem D, Melamed Y. Effect of combined recompression and air, oxygen, or heliox breathing on air bubbles in rat tissues. J Appl Physiol 2001; 90:1639–47.
12. Hyldegaard O, Madsen J. Effect of hypobaric air, oxygen, heliox (50:50), or heliox (80:20) breathing on air bubbles in adipose tissue. J Appl Physiol 2007; 103:757–62.
13. Hyldegaard O, Moller M, Madsen J. Effect of He-O2, O2, and N2O-O2 breathing on injected bubbles in spinal white matter. Undersea Biomed Res 1991; 18:361–71.
14. Madsen J, Malchow-Moller A, Waldorff S. Continuous estimation of adipose tissue blood flow in rats by 133Xe elimination. J Appl Physiol 1975; 39:851–6.
15. Muehlberger PM, Pilmanis AA, Webb JT, Olson JE. Altitude decompression sickness symptom resolution during descent to ground level. Aviat Space Environ Med 2004; 75:496–9.
16. Olson RM, Krutz RW, Jr. Significance of delayed symptom onset and bubble growth in altitude decompression sickness. Aviat Space Environ Med 1991; 62:296–9.
17. Randsoe T, Hyldegaard O. Effect of oxygen breathing and perfluorocarbon emulsion treatment on air bubbles in adipose tissue during decompression sickness. J Appl Physiol 2009; 107:1857–63.
18. Randsoe T, Hyldegaard O. Effect of oxygen breathing on micro oxygen bubbles in nitrogen-depleted rat adipose tissue at sea level and 25 kPa altitude exposures. J Appl Physiol 2012; 113:426–33.
19. Randsoe T, Kvist TM, Hyldegaard O. Effect of oxygen and heliox breathing on air bubbles in adipose tissue during 25-kPa altitude exposures. J Appl Physiol 2008; 105:1492–7.
20. Rasband W. Image [computer program]. Image Processing and Analysis (version 1.61). National Institutes of Health, Services Research Branch, National Institute of Mental Health. Washington, DC: National Institutes of Health; 1996. Retrieved February 2010 from http://rsb.info.nih.gov/nih-image/download.html.
21. Spiess BD. Perfluorocarbon emulsions as a promising technology: a review of tissue and vascular gas dynamics. J Appl Physiol 2009; 106:1444–52.
22. SPSS [computer program]. Statistical Package of the Social Sciences. Chicago, IL: SPSS; 1998.
23. Van Liew HD, Burkard ME. Simulation of gas bubbles in hypobaric decompressions: roles of O2, CO2, and H2O. Aviat Space Environ Med 1995; 66:50–5.
24. Van Liew HD, Conkin J, Burkard ME. The oxygen window and decompression bubbles: estimates and significance. Aviat Space Environ Med 1993; 64:859–65.
25. Van Liew HD, Hlastala MP. Influence of bubble size and blood perfusion on absorption of gas bubbles in tissues. Respir Physiol 1969; 7:111–21.
26. Weathersby PK, Homer LD. Solubility of inert gases in biological fluids and tissues: a review. Undersea Biomed Res 1980; 7:277–96.
27. Webb JT, Pilmanis AA, O'Connor RB. An abrupt zero-preoxygenation altitude threshold for decompression sickness symptoms. Aviat Space Environ Med 1998; 69:335–40.
28. Ganong WF. Pulmonary function. In: Review of medical physiology. Los Altos: Lange Medical Publications; 1983.
29. Wisløff U, Richardson RS, Brubakk AO. Exercise and nitric oxide prevent bubble formation: a novel approach to the prevention of decompression sickness? J Physiol 2004; 555:825–9.